

Novel Moving Steady-State Visual Evoked Potential Stimulus to Assess Afferent and Efferent Dysfunction in Multiple Sclerosis

Masaki Nakanishi¹, Senior Member, IEEE, Annalise Miner,
Tzyy-Ping Jung², Fellow, IEEE, and Jennifer Graves

Abstract—Afferent and efferent visual dysfunction are prominent features of multiple sclerosis (MS). Visual outcomes have been shown to be robust biomarkers of the overall disease state. Unfortunately, precise measurement of afferent and efferent function is typically limited to tertiary care facilities, which have the equipment and analytical capacity to make these measurements, and even then, only a few centers can accurately quantify both afferent and efferent dysfunction. These measurements are currently unavailable in acute care facilities (ER, hospital floors). We aimed to develop a moving multifocal steady-state visual evoked potential (mfSSVEP) stimulus to simultaneously assess afferent and efferent dysfunction in MS for application on a mobile platform. The brain-computer interface (BCI) platform consists of a head-mounted virtual-reality headset with electroencephalogram (EEG) and electrooculogram (EOG) sensors. To evaluate the platform, we recruited consecutive patients who met the 2017 MS McDonald diagnostic criteria and healthy controls for a pilot cross-sectional study. Nine MS patients (mean age 32.7 years, SD 4.33) and ten healthy controls (24.9 years, SD 7.2) completed the research protocol. The afferent measures based on mfSSVEPs showed a significant difference between the groups (signal-to-noise ratio of mfSSVEPs for controls: 2.50 ± 0.72 vs. MS: 2.04 ± 0.47) after controlling for age ($p = 0.049$). In addition, the moving stimulus successfully induced smooth pursuit movement that can be measured by the EOG signals. There was a trend for worse smooth pursuit tracking in cases vs. controls, but this did not reach nominal statistical significance in this small pilot sample. This study introduces a novel moving mfSSVEP stimulus for a BCI platform to evaluate neurologic visual function. The moving stimulus showed a reliable capability to assess both afferent and efferent visual functions simultaneously.

Manuscript received 11 July 2022; revised 14 October 2022 and 12 December 2022; accepted 27 December 2022. Date of publication 8 February 2023; date of current version 16 February 2023. This work was supported by the University of California San Diego Galvanizing Engineering in Medicine Program. (Corresponding author: Masaki Nakanishi.)

This work involved human subjects or animals in its research. Approval of all ethical and experimental procedures and protocols was granted by the University of California San Diego Human Research Protections Program.

Masaki Nakanishi and Tzyy-Ping Jung are with the Swartz Center for Computational Neuroscience, Institute for Neural Computation, University of California San Diego, La Jolla, CA 92093 USA (e-mail: masaki@sccn.ucsd.edu; jung@sccn.ucsd.edu).

Annalise Miner and Jennifer Graves are with the Department of Neuroscience, University of California San Diego, La Jolla, CA 92093 USA (e-mail: aeminer@health.ucsd.edu; jgraves@health.ucsd.edu).

Digital Object Identifier 10.1109/TNSRE.2023.3243554

Index Terms—Afferent and efferent visual pathway, electroencephalogram (EEG), electrooculogram (EOG), multifocal steady-state visual evoked potential (mfSSVEP), multiple sclerosis (MS), virtual reality headset.

I. INTRODUCTION

ONE of the greatest unmet needs in multiple sclerosis (MS) research and clinical care is the ability to quantify disease burden with highly reproducible and rater-independent methods. Significant advancements have been made in measuring visual dysfunction through the use of low-contrast letter acuity measures, visual evoked potentials (VEP), optical coherence tomography (OCT), and efferent oculometrics, but these tools are not in widespread use in most MS clinics and often require support from those with subspecialty training in neuro-ophthalmology [1]. Most of the equipment is cumbersome and immovable. The functional vision measures also typically require performing a correction of refractive error, which most neurologists are not equipped to provide in their offices.

Despite the difficulty of conducting extensive, systematic visual testing in neurology clinics or acute care settings, the visual system has demonstrated an exceptional ability to detect demyelinating injury even in those who have no clinical symptoms. Standard full-field VEP has been used to support the diagnosis of MS for over 50 years [2], [3]. In young patients with MS, without any detectable exam finding abnormalities, latency delays can be seen for saccadic (fast) eye movements that distinguish these patients from healthy controls [4]. Disruption of smooth pursuit eye movements also distinguishes MS eyes from controls [5]. The current understanding of the quantitative relationships between structure and function in the visual system far surpasses that of other central nervous system pathways. Thus, the afferent and efferent visual pathways are well poised to serve as a model system of injury and repair for therapeutic investigations and clinical monitoring in MS [6].

The majority of MS patients are not diagnosed or cared for in clinic settings with advanced visual function testing facilities. A mobile platform that does not require dedicated room space or a trained technician, such as the one proposed here, would enable more widespread use of quantitative afferent/efferent vision testing in acute care settings and non-tertiary care centers.

Efferent visual function testing is currently only used in observational research settings. Despite its proven ability to

detect dysfunction, quantification of dysfunction has not been brought to the clinic or trial setting. This situation is largely due to the lack of technical expertise and immovable equipment needed to perform these measurements. As an example, one of the most commonly used platforms for MS studies requires the clinician, technician or researcher to write their own software, which is not practical for neurologists in private practice. By developing commercial-grade algorithms, we will remove the need for signal-processing expertise. The use of a headset platform will allow the testing to be brought to the patient rather than having to burden the patient with a trip to an offsite research lab. Removing these critical barriers will facilitate the use of efferent visual outcome measures in clinical trials and clinic settings.

Recently, brain-computer interfaces based on multi-focal steady-state VEP (mfSSVEP) have been used to objectively assess visual-field deficits in glaucoma patients [7]. In contrast to transient (i.e., standard) VEPs, steady-state VEPs (SSVEPs) are elicited by rapid flickering stimulation, producing a brain response characterized by a quasi-sinusoidal waveform that has frequency components with constant amplitude and phase [8]. The technique is faster than standard VEPs and less susceptible to artifacts produced by blinking and eye movements as well as electromyographic noise contamination, and it may present a better signal-to-noise ratio [9], [10], [11], [12], [13], [14]. The current study builds on the prior work in glaucoma by adding a moving multi-focal SSVEP (mfSSVEP) stimulus for assessing both afferent and efferent visual function simultaneously. The MSight BCI platform piloted in this study will greatly facilitate research on the correlations between the afferent and efferent measures in neurological disease and support the development of new and novel indices of MS-related visual dysfunction. We hypothesized that SSVEP amplitudes across the frequencies assessed would be lower compared to control subjects given the high prevalence of both clinical and subclinical afferent injury in MS. We also hypothesized reduced fidelity of stimulus tracking in the efferent measure based on high rates of efferent visual dysfunction even in those with mild disease course.

II. METHODS

A. Participants

We offered enrollment to consecutive patients who attended the University of California San Diego (UCSD) MS Center. Participants with MS had to meet the updated 2017 McDonald criteria for MS [15]. The included participants were exposed to a variety of MS disease modifying medications including oral (e.g., dimethyl fumarate, fingolimod) and infusion (e.g., ocrelizumab) medications. Age similar healthy controls had no history of neurological or ophthalmological disease. The study was approved by UCSD Human Research Protections Program and all participants provided informed written consent.

B. Visual Stimulus

Multi-focal visual stimuli consisting of two patterns of 20 sectors in three concentric rings (subtending 8.4° , 21° , and 35° of the visual field) and moving in 15° -wide 2-D

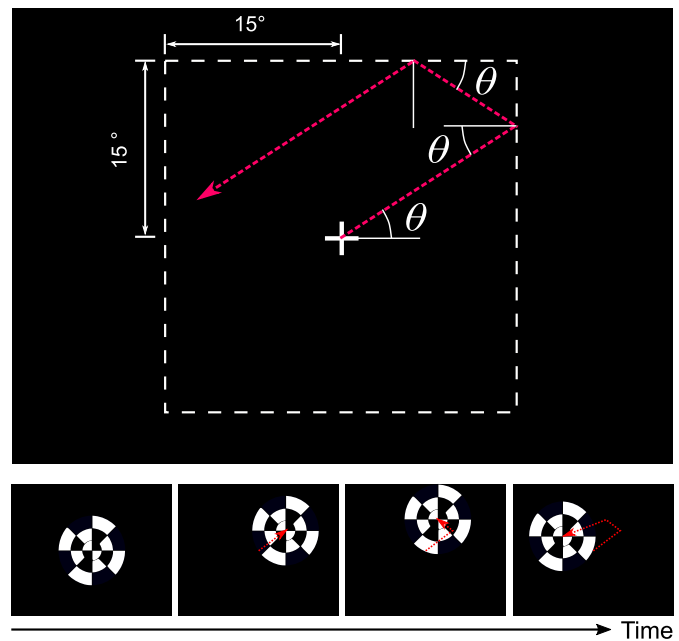


Fig. 1. A moving multi-focal stimulus. (Top) The stimulus was presented at the center of a screen and started to move at a constant speed with an angle θ assigned randomly in a 15° -wide 2-D space. To avoid visually-crowded illustration, the fixation point was depicted rather than the multi-focal stimulus in the figure. (Bottom) Participants fixed their gaze at the center of the stimulus so that it simultaneously elicits multi-focal steady-state visual evoked potentials (mfSSVEPs) and smooth eye movements.

space at a constant speed [8] were implemented and presented on a Samsung Odyssey + head-mounted display (HMD). Different frequencies were assigned to each sector, ranging from 8 to 11.8 Hz with a frequency interval of 0.2 Hz. To enhance the signal-to-noise ratio (SNR) in eliciting mfSSVEPs, the platform uses a frequency-approximation approach to render flexible frequencies with a variable number of frames in a stimulating period [16], [17]. Two patterns (A and B) of visual stimuli, each with 10 of 20 sectors flickered concurrently, were presented separately, to facilitate the calculation of the SNR (see *II-D Data Analysis*). For example, the stimulus pattern A contained 8 to 11.6 Hz with a 0.4 Hz interval and the stimulus pattern B contained 8.2 to 11.8 Hz with a 0.4 Hz interval. The fixation target moves in 2-D space at $v = 60^\circ/s$ rendered randomly and smoothly on the screen of the HMD (Fig. 1). At the beginning of each trial, a 2-D moving angle θ was assigned, and the horizontal and the vertical moving speeds were determined based on the angle. For example, horizontal and vertical speeds can be determined as $v\cos(\theta)$ and $v\sin(\theta)$, respectively. Once the stimulus reached to one of the 15° -wide boundaries in four directions, the moving direction was flipped as shown in Fig. 1.

C. Data Acquisition

EEG and electrooculogram (EOG) data were measured using a BioSemi ActiveTwo EEG system (BioSemi, Inc.). EEG data were recorded with nine Ag/AgCl Electrodes covering the occipital area and an additional one at Cz. EOG electrodes were placed above the superior orbit and below the inferior



Fig. 2. Experimental environment. Participants fixed their gaze at the center of the stimulus so that it simultaneously elicits multi-focal steady-state visual evoked potentials (mfSSVEPs) and saccadic eye movements.

orbit for vertical eye movement and to the left of the left and right of each eye for horizontal eye movement. The HMD was placed on top of the electrode cap (Fig. 2). The data were digitized with common mode sense (CMS) and driven right leg (DRL) electrodes at a sampling rate of 2,048 Hz. Event triggers that indicated the onsets of visual stimulation and horizontal and vertical stimulus position were sent through the LabStreamingLayer (LSL) [18] to the EEG system. The participants were asked to sit in a comfortable chair and gaze at a red dot located in the center of the moving visual stimuli. They were also instructed to avoid eye blinking during the 5-second visual stimulation. The experiment consisted of three sessions with stimulus A-pattern and three sessions with stimulus B-pattern for each eye. Each session per eye contained 30 6-second trials, including 5 seconds of visual stimulation followed by a 1-second short break, totaling 3 minutes. In sum, each participant performed 360 trials (i.e., 2 eyes \times 2 stimulus patterns \times 3 sessions \times 30 trials/session) of the gazing task.

D. Data Analysis

EEG data were first resampled to 256 Hz and re-referenced to the Cz channel. Then, data epochs composed of 9-channel 5-second mfSSVEPs were extracted from the continuous EEG data according to the event markers. Considering a latency delay in the visual system [19], the data epochs were extracted in [0.14 5.14] s, where the time zero indicated stimulus onsets. Each EEG epoch was band-pass filtered using a Chebyshev Type I filter created with MATLAB's *cheb1ord()* and *cheby()* functions. The filter has less than 3 dB of ripple in the passband between 6 and 90 Hz, a stopband that attenuated by 35 dB below 4 Hz and above 100 Hz to preserve the components at the frequencies of interest (i.e., 8, 8.2, . . . , 11.8 Hz with an interval of 0.2 Hz) and their harmonic components [20]. Zero-phase forward and reverse filtering was implemented using the *filtfilt()* function in Matlab. As an afferent measure, we employed the SNR of mfSSVEPs which was defined as the ratio of the signal power induced by the stimuli to that of spontaneous activity [17], [21]. Having the two stimulus patterns (i.e., A and B), the signals and noises can be defined as the components corresponding to the frequencies that flickered in a pattern and that did not flicker in the other pattern, respectively. Therefore, it can be computed as follows:

$$\text{SNR} = \frac{\sum_{f \in f_t} F(f)}{\sum_{f \in f_{nt}} F(f)}, \quad (1)$$

where $F(f)$ indicates the amplitude spectrum at a frequency of f Hz computed by discrete Fourier transform (DFT), and f_t and f_{nt} are subsets of stimulus frequencies ranging from 8.0 to 11.8 Hz containing target and non-target frequencies that are contained in each pattern of visual stimulus (e.g., 8.0, 8.4, . . . , 11.6 Hz are target and 8.2, 8.6, . . . , 11.8 Hz are non-target frequencies for pattern A). The SNR was quantified for each eye on each participant. To compute an SNR, we first took an average of 90 5-s data epochs on each condition (i.e., eye and stimulus pattern), obtained amplitude spectra by applying DFT to the averaged waveforms, and then computed the eq (1) using the spectra corresponding to the stimulus patterns A and B. The SNR defined here indicates the changes of frequency components in EEG due to the visual stimulation, which is suitable to measure the abnormality in afferent visual pathway [17].

EOG data were also resampled to 256 Hz and converted to vertical and horizontal EOG (vEOG and hEOG) by subtracting the signal obtained from the electrodes placed above superior orbit and below inferior orbit and right and left of each eye, respectively. However, the electrode placed above the superior orbit interfered with the HMD, contaminating the EOG data with interference noises. As a result, vEOG measurements were excluded from the following analysis. The data were then epoched according to the event triggers. To quantify the participants' efferent tracking function, correlation coefficients between the amplitude of hEOG data and the horizontal trajectory of the visual stimulus were computed as eye-tracking performance.

One-way analysis of covariances (ANCOVAs) were conducted to determine statistically significant differences between the MS participants and the healthy controls on the SNR of mfSSVEPs and the eye-tracking performance controlling for age. In other words, the participants' age was the covariate in the ANCOVA.

III. RESULTS

We recruited nine MS participants (mean age: 32.7 ± 4.33 yrs., 66.6 % female) and ten healthy controls (mean age: 24.9 ± 7.2 yrs., 80 % female). The MS patients exhibited a wide range of disability accumulation, as measured by the Expanded Disability Status Scale (EDSS) scores. MS subjects had EDSS scores from 0 (no disability) to 6.5 (needing a walker for ambulation). The averaged disease duration was 8.8 years ranging from 0.9 to 24.6 years. Eight MS participants had a history of clinical optic neuritis and no patients had history of an overt clinical efferent abnormality on a bedside exam.

Fig. 3 illustrates examples of the amplitude spectra of mfSSVEPs and EOG-based horizontal eye-tracking data collected from a healthy control and an MS participant. Each amplitude spectrum was obtained by combining the spectra corresponding to the two visual stimulus patterns (i.e., (a) and (b)). More specifically, the maximum values at each frequency bins between the two spectra were obtained and used to draw the final spectrum shown in Fig. 3(a). As shown in the figure, the MS patient clearly showed degraded mfSSVEP amplitude across the frequency spectrum

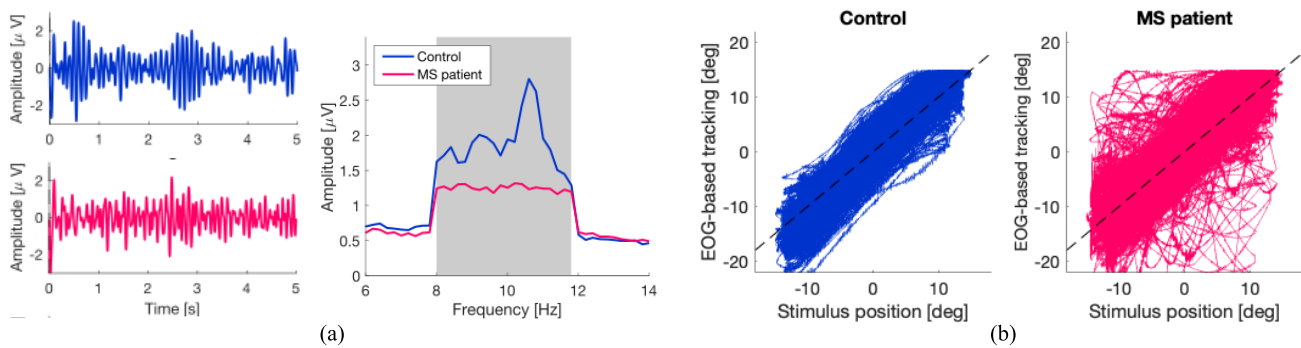


Fig. 3. Examples of (a) the time-series and amplitude spectra of mfSSVEPs and (b) EOG-based eye tracking data collected from a healthy participant and a MS participant. The frequency range highlighted in gray indicates the frequency range of stimulus frequencies (i.e., 8 - 11.8 Hz).

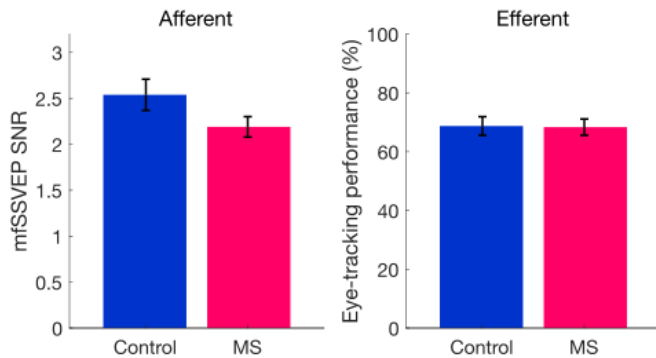


Fig. 4. Averaged mfSSVEP SNR (left) and eye-tracking performance (right) across participants in each group. The error bars indicate standard errors.

and weakly-correlated eye trajectory with the moving stimulus compared with the healthy control. In Fig. 3(b), the stimulus position and EOG-based eye trajectory were plotted in 2-D spaces. The control eye was able to closely track the stimulus while the MS eye had evident departures from the stimulus position.

Fig. 4 shows the averaged mfSSVEP signal-to-noise ratio (SNR) and eye-tracking performance across eyes in each group. The mean SNR of mfSSVEPs in the control and MS groups were 2.54 ± 0.76 and 2.19 ± 0.47 , respectively. The one-way ANCOVA showed that the SNRs of the mfSSVEP in the control group were significantly higher than those in the MS group after controlling for participants' age ($F(1,34) = 4.18$, $p = 0.049$). The mean eye-tracking performance in the control and MS groups were 68.71 ± 14.16 and 68.33 ± 11.75 , respectively. Across the MS and controls groups, there was no statistically significant difference in the mean eye-tracking performance after controlling for participants' age ($F(1,34) = 0.01$, $p = 0.753$) in this pilot sample size, despite some extreme differences for some MS participants (Figure 3).

IV. DISCUSSION

This study provides preliminary validation of this VR BCI-based assessment of MS-related visual dysfunction and introduced a novel moving evoked potential stimulus. While afferent and efferent measures have independently shown validity as disease burden outcomes in MS and other neurological diseases, this is the first use of a moving evoked

potential stimulus to simultaneously stimulate both visual systems [22], [23], [24]. This pilot paradigm integrated an EEG headset with an HMD to create a portable data collection method and applied a moving mfSSVEP stimulus to concurrently assess both afferent and efferent visual pathways in MS patients. Our results demonstrated that mfSSVEP SNR was significantly lower in MS patients than in healthy control eyes, suggesting that this approach can be used to assess afferent visual dysfunction in MS eyes.

These measures provide valuable insight and potential biomarkers for sub-clinical disease activity in the MS population. Additionally, this integrated headset's ability to collect multiple measures of visual function underlines its use as an efficient and transportable tool for tracking disease progression.

The efferent measures based on the hEOG-based eye-tracking performance showed a trend between the two experimental groups, but not a nominally statistically significant difference. The small sample size of this pilot study may be one factor contributing to this. A few participants had apparent subclinical abnormalities on this efferent testing and this pilot test demonstrated the ability to elicit eye movement responses with the novel stimulus. Participants recruited did not have overt clinical efferent dysfunction on bedside exam, which may have impacted the lack of nominal statistical significance in this small sample size. It could also reflect the fact that EOG data were largely contaminated by the interferences from the head-mounted display because it was placed on top of the electrodes. Removal of the vEOG data due to technical artifact may have obscured the ability to measure the differences in efferent features between MS participants and healthy controls. Newer VR headset models include a built-in video-based eye-tracker (e.g. HTC Vive Pro Eye); in the future, using such devices to precisely assess the efferent visual pathway would be preferable and will be pursued for the advancement of this platform. The overall results of this study demonstrate the importance of re-examining these findings with a larger sample size and updated technology in order to establish validity and revisit the significance of efferent visual pathway measures. It will also be imperative to address potential longitudinal changes in these measures in both MS patients and healthy controls, to evaluate the device's applicability as a reliable marker of MS disease progression.

V. CONCLUSION

This study uses a virtual reality headset with a moving visual flicker stimulus to simultaneously assess afferent and efferent visual functions. The results showed that the proposed mobile platform could induce and measure both mfSSVEPs and smooth pursuit behavior in healthy controls and MS patients. In particular, the SNR of mfSSVEPs in the MS patients was significantly lower than that in the healthy controls, indicating a degraded afferent visual function in the MS patients. The proposed protocol has a great potential to facilitate research and the development of a novel diagnostic tool for MS-related visual dysfunction.

ACKNOWLEDGMENT

The authors would like to thank the generous participants who donated their time for this study.

REFERENCES

- [1] J. S. Graves et al., "Leveraging visual outcome measures to advance therapy development in neuroimmunologic disorders," *Neurol. Neuroimmunology Neuroinflammation*, vol. 9, no. 2, p. e1126, Mar. 2022.
- [2] L. Leocani, S. Guerrieri, and G. Comi, "Visual evoked potentials as a biomarker in multiple sclerosis and associated optic neuritis," *J. Neuro-Ophthalmology*, vol. 38, no. 3, pp. 350–357, Sep. 2018.
- [3] J. L. Barton, J. Y. Garber, A. Klistorner, and M. H. Barnett, "The electrophysiological assessment of visual function in multiple sclerosis," *Clin. Neurophysiol. Pract.*, vol. 4, pp. 90–96, May 2019.
- [4] A. Yousef et al., "Subclinical saccadic eye movement dysfunction in pediatric multiple sclerosis," *J. Child Neurol.*, vol. 34, no. 1, pp. 38–43, Jan. 2019.
- [5] T. Rempé et al., "Quantification of smooth pursuit dysfunction in multiple sclerosis," *Multiple Sclerosis Rel. Disorders*, vol. 54, Sep. 2021, Art. no. 103073.
- [6] J. Graves and L. J. Balcer, "Eye disorders in patients with multiple sclerosis: Natural history and management," *Clin. Ophthalmol.*, vol. 4, pp. 1409–1422, Dec. 2010.
- [7] M. Nakanishi et al., "Detecting glaucoma with a portable brain-computer interface for objective assessment of visual function loss," *JAMA Ophthalmol.*, vol. 135, no. 6, pp. 550–557, Jun. 2017.
- [8] F. B. Vialatte, M. Maurice, J. Dauwels, and A. Cichocki, "Steady-state visually evoked potentials: Focus on essential paradigms and future perspectives," *Prog. Neurobiol.*, vol. 90, pp. 418–438, Apr. 2010.
- [9] A. M. Norcia, L. G. Appelbaum, J. M. Ales, B. R. Cottreau, and B. Rossion, "The steady-state visual evoked potential in vision research: A review," *J. Vis.*, vol. 15, no. 6, p. 4, May 2015.
- [10] S. N. Abdullah, N. Aldahlawi, Y. Rosli, Vaegan, M. Y. Boon, and T. Maddess, "Effect of contrast, stimulus density, and viewing distance on multifocal steady-state visual evoked potentials (MSVs)," *Investigative Ophthalmol. Visual Sci.*, vol. 53, no. 9, pp. 5527–5535, Aug. 2012.
- [11] S. N. Abdullah, Vaegan, M. Y. Boon, and T. Maddess, "Contrast-response functions of the multifocal steady-state VEP (MSV)," *Clin. Neurophysiol.*, vol. 123, no. 9, pp. 1865–1871, Sep. 2012.
- [12] G. G. Celesia, M. Brigell, R. Gunnink, and H. Dang, "Spatial frequency evoked visuograms in multiple sclerosis," *Neurology*, vol. 42, no. 5, pp. 1067–1070, May 1992.
- [13] S. Tobimatsu, S. Tashima-Kurita, M. Nakayama-Hiromatsu, and M. Kato, "Clinical relevance of phase of steady-state VEPs to P100 latency of transient VEPs," *Electroencephalogr. Clin. Neurophysiol./Evoked Potentials Sect.*, vol. 80, no. 2, pp. 89–93, Mar. 1991.
- [14] H. Abe, S. Hasegawa, M. Takagi, T. Yoshizawa, and T. Usui, "Temporal modulation transfer function of vision by pattern visual evoked potentials in patients with optic neuritis," *Ophthalmologica*, vol. 207, no. 2, pp. 94–99, 1993.
- [15] A. J. Thompson et al., "Diagnosis of multiple sclerosis: 2017 revisions of the McDonald criteria," *Lancet Neurol.*, vol. 17, no. 2, pp. 162–173, Feb. 2018.
- [16] Y. Wang, Y.-T. Wang, and T.-P. Jung, "Visual stimulus design for high-rate SSVEP BCI," *Electron. Lett.*, vol. 46, no. 15, pp. 1057–1058, 2010.
- [17] M. Nakanishi, Y. Wang, Y.-T. Wang, Y. Mitsukura, and T.-P. Jung, "Generating visual flickers for eliciting robust steady-state visual evoked potentials at flexible frequencies using monitor refresh rate," *PLoS ONE*, vol. 9, no. 6, Jun. 2014, Art. no. e99235.
- [18] C. A. Kothe and S. Makeig, "BCILAB: A platform for brain-computer interface development," *J. Neural Eng.*, vol. 10, no. 5, 2013, Art. no. 056014.
- [19] Y. Wang, X. Gao, and S. Gao, "Computational modeling and application of steady-state visual evoked potentials in brain-computer interfaces," *Sci. Suppl.*, vol. 350, no. 6256, pp. 43–46, 2015.
- [20] X. Chen, Y. Wang, M. Nakanishi, X. Gao, T.-P. Jung, and S. Gao, "High-speed spelling with a noninvasive brain-computer interface," *Proc. Nat. Acad. Sci. USA*, vol. 112, no. 44, pp. E6058–E6067, Nov. 2015.
- [21] Y. Wang, R. Wang, X. Gao, B. Hong, and S. Gao, "A practical vep-based brain-computer interface," *IEEE Trans. Neural Syst. Rehabil. Eng.*, vol. 14, no. 2, pp. 234–239, Feb. 2006.
- [22] M. Jozefowicz-Korczynska and A. M. Pajor, "Evaluation of the smooth pursuit tests in multiple sclerosis patients," *J. Neurol.*, vol. 258, no. 10, pp. 1795–1800, Oct. 2011.
- [23] N. Lizak, M. Clough, L. Millist, T. Kalincik, O. B. White, and J. Fielding, "Impairment of smooth pursuit as a marker of early multiple sclerosis," *Frontiers Neurol.*, vol. 7, p. 206, Nov. 2016.
- [24] D. B. Liston, L. R. Wong, and L. S. Stone, "Oculometric assessment of sensorimotor impairment associated with TBI," *Optometry Vis. Sci.*, vol. 94, no. 1, pp. 51–59, 2017.